# Mineralogical Asbestos Assessment in the Southern Apennines (Italy): A Review

**Maria Carmela Dichicco [1], Michele Paternoster [1,2], Giovanna Rizzo [1,*] and Rosa Sinisi [1]**

[1]    Department of Sciences, University of Basilicata, Campus di Macchia Romana, Viale dell'Ateneo Lucano 10, 85100 Potenza, Italy; maria.dichicco@unibas.it (M.C.D.); michele.paternoster@unibas.it (M.P.); rosa.sinisi@unibas.it (R.S.)

[2]    Istituto Nazionale di Geofisica e Vulcanologia, Sezione di Palermo, Via Ugo La Malfa 153, 90146 Palermo, Italy

*    Correspondence: giovanna.rizzo@unibas.it; Tel.: +39-0971-20-5833

**Abstract:** This paper deals with petrography and mineralogy of serpentinitic rocks occurring in the Southern Apennines (Italy) with the aim to review the already available literature data and furnish new details on asbestos minerals present in the studied area. Two sites of Southern Italy were taken into account: the Pollino Massif, at the Calabrian-Lucanian border, and the surroundings of the Gimigliano and Mt. Reventino areas where serpentinites of Frido Unit are mainly exposed. Textural and mineralogical features of the studied rocks point to a similar composition for both sites including asbestos minerals such as chrysotile and tremolite-actinolite series mineral phases. Only in the Pollino Massif serpentinites edenite crystals have been detected as well; they are documented here for the first time. This amphibole forms as fibrous and/or prismatic crystals in aggregates associated with serpentine, pyroxene, and calcite. Metamorphism and/or metasomatic alteration of serpentinites are the most probable processes promoting the edenite formation in the Southern Apennine ophiolitic rocks.

**Keywords:** asbestos' minerals; edenite; serpentinites; Southern Italy

## 1. Introduction

In the last decade, many researchers have focused on serpentinites cropping out in the ophiolitic sequences and have aimed to assess and monitor their potential as asbestos-bearing lithotypes, since asbestos occurrence in mafic and ultramafic rocks that undergo ocean floor metamorphism is relatively common [1–4]. In Italy, the occurrence of these rocks is documented both in the Alps and Apennines. These outcrops extend from the Ligurian-Piedmont through the Tuscan-Emilian Apennines as far as Val Tiberina and continue, in disjointed groupings, to the Calabrian-Lucanian Apennines [5].

As is known, the definition of asbestos used by regulatory agencies [6] for identification includes the following six mineral species: chrysotile, crocidolite, tremolite, actinolite, amosite, and anthophyllite [7]. Among these minerals, only chrysotile is a sheet silicate; the other minerals are included within the amphibole supergroup. Silicate minerals belonging to the serpentine and amphibole groups are flexible, heat-resistant, and chemically inert. These minerals usually occur with an elongated and/or bladed prismatic habit, although they may be acicular or fibrous as well. In the European countries, fibers having a length $\geq 5$ μm, a width $<3$ μm, and an aspect ratio $>3$ are defined as "asbestos" by Directive 2003/18/CE.

Asbestos is classified as a carcinogen material of Category 1 by the world health authorities [8]. Several authors ascribe the fibers' toxicity to their morphology and size, chemical-physical

characteristics, surface reactivity, and biopersistence [9]. It is known that the presence of impurities (i.e., Fe, Ni, and Ti) in the ideal chemical composition in asbestos fibers, even in small amounts, affects their chemical and physical properties, size, and shape [10–13]. Moreover, according to in vitro studies on biological-system–mineral interactions, both characteristics (impurities and size) are considered to be responsible for its pathological effects [14,15].

In this paper, we present data related to petrography and mineralogy of serpentinites in representative sites at the Pollino Massif (Calabrian-Lucanian boundary) and Gimigliano-Mt. Reventino (Sila Piccola, Northern Calabria), with the principal aim to review the main modes of occurrence of asbestos minerals in the Southern Apennines.

## 2. Ophiolitic Sequences in Southern Italy

The Southern Apennines is a fold-and-thrust chain developed between the Upper Oligocene and the Quaternary during the convergence between the African and European plates [16–18]. The ophiolitic sequences incorporated in the Southern Apennine chain are related to the northwest subduction of the oceanic lithosphere pertaining to the Ligurian sector (divided in the Frido Unit and North Calabrian Unit) of the Jurassic Western Tethys. They crop out in the northeastern slope of the Pollino Ridge, along with the Calabria-Lucanian border zone, and in the Gimigliano-Mt. Reventino Unit (Sila Piccola, Southern Italy) (Figure 2). At the Calabrian-Lucanian boundary, the investigated sites are on well-exposed outcrops along road cuts, active and inactive quarries or in the proximity of villages (Pietrapica quarry, Timpa Castello quarry, Fagosa quarry, and Fosso Arcangelo, San Severino Lucano, Rovine Convento Sagittale localities, Mt. Nandiniello and Ghiaia quarry) (Figure 1), whereas close to the Gimigliano town the outcrops are in correspondence of quarries at Sila Piccola, Northern Calabria [5,19–21].
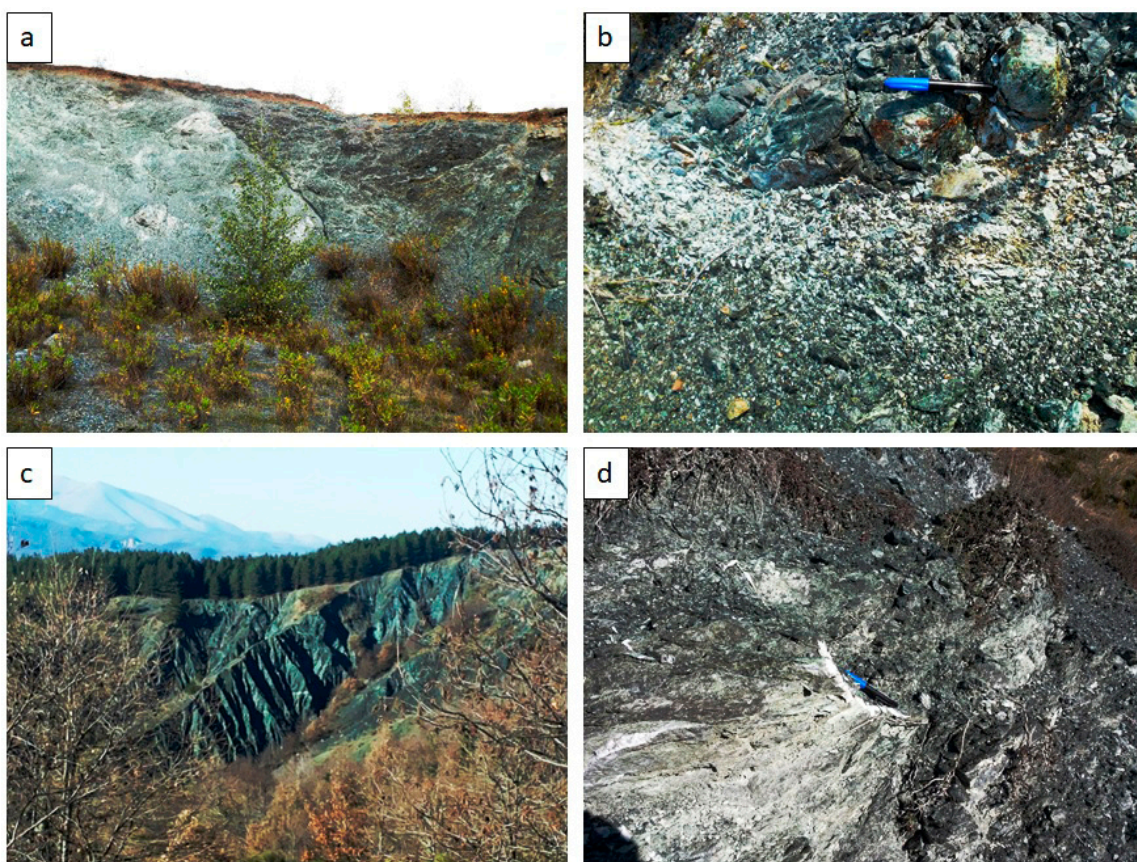


**Figure 1.** Serpentinite outcrops of the Pollino Massif: (**a**) Fagosa quarry, (**b**) Mt. Nandiniello, (**c**) Fosso Arcangelo site, and (**d**) San Severino Lucano site.

In the following sections, details on geological setting and formations of both sites are presented.

### 2.1. The Pollino Massif Serpentinites

According to several authors [22–25], the Frido Unit forms the uppermost thrust sheet of southern Apennines and tectonically overlies the North Calabrian Units, which in turn are split in different thrust sheets [25]. The Frido Unit is characterized by HP/LT metamorphic sequences developed between Upper Jurassic to the Upper Oligocene [26–29] and references therein. The ophiolitic rocks in the Frido Unit, from the bottom to the top, consist of tectonized serpentinite [30–35], metabasalt [36], metagabbro, metapillow lavas [37], dismembered metadoleritic and rodingite dykes [28,38–40], and sedimentary cover [41]. The serpentinites are englobed in tectonic slices and are associated with metadolerite dykes and continental crust rocks that mainly consist of weathered granofels, garnet gneiss, garnet–biotite gneiss, leucocratic biotite gneiss, and lenticular bodies of amphibolite [42]. As suggested by Knott [23], the Frido Unit underwent a polyphase blueschist to greenschist facies metamorphism developed in the deeper portions of the Liguride accretionary wedge.

In the Pollino Massif, the serpentinite rocks are cataclastic and massive. Cataclastic serpentinites show a high degree of fracturing and deformation. The millimeter to centimeter fractures are almost filled by exposed white and grey fibrous minerals [30,32,33]. Fibers occur as both large and elongate minerals developed over slickensided surfaces and/or as very fine-grained phases pervading the whole rock. Massive serpentinites show a low fracturing and deformation without exposed fibers.

### 2.2. The Gimigliano-Mt. Reventino Serpentinites

The Gimigliano-Mt. Reventino (Sila Piccola, Figure 2) occurs in the northern sector of the Calabrian-Peloritan Orogen [43,44]. According to Ogniben [45,46], the Northern Calabria sector consists of three main tectonic complexes: the Apennine Units Complex, at the bottom, made up of Mesozoic sedimentary and metasedimentary terranes; the allochthonous Alpine Liguride Complex, in the intermediate position, consisting of a series of Cretaceous-Paleogene metamorphic units that include metapelites, ophiolites, and carbonates; the Calabride Complex, at the top, with granites, gneisses, and metasedimentary deposits derived from Hercynian and pre-Hercynian terranes. The Mt. Reventino area is characterized mainly by lenses of metabasalts and serpentinites limited by low angle tectonic systems, with metapelites, metalimestones, and metarenites of uncertain ages of the Frido Unit (Liguride Complex). The massive-banded metabasalts and serpentinites lenses constitute the upper part of Mt. Reventino [43]. In the ophiolitic bodies, ascribed to the Liguride Complex of oceanic derivation [46–49], the serpentinites occupy the cores of the major tight folds and are partially or completely surrounded by isolated bodies of metabasalts and subordinate metadolerites [43]. In the Gimigliano-Mt. Reventino two different types of serpentinites occur as foliated and massive rocks. Mostly dark green serpentinites crop out as massive bodies that only sometimes are weakly foliated and cut by serpentine and calcite veins [5,19–21].
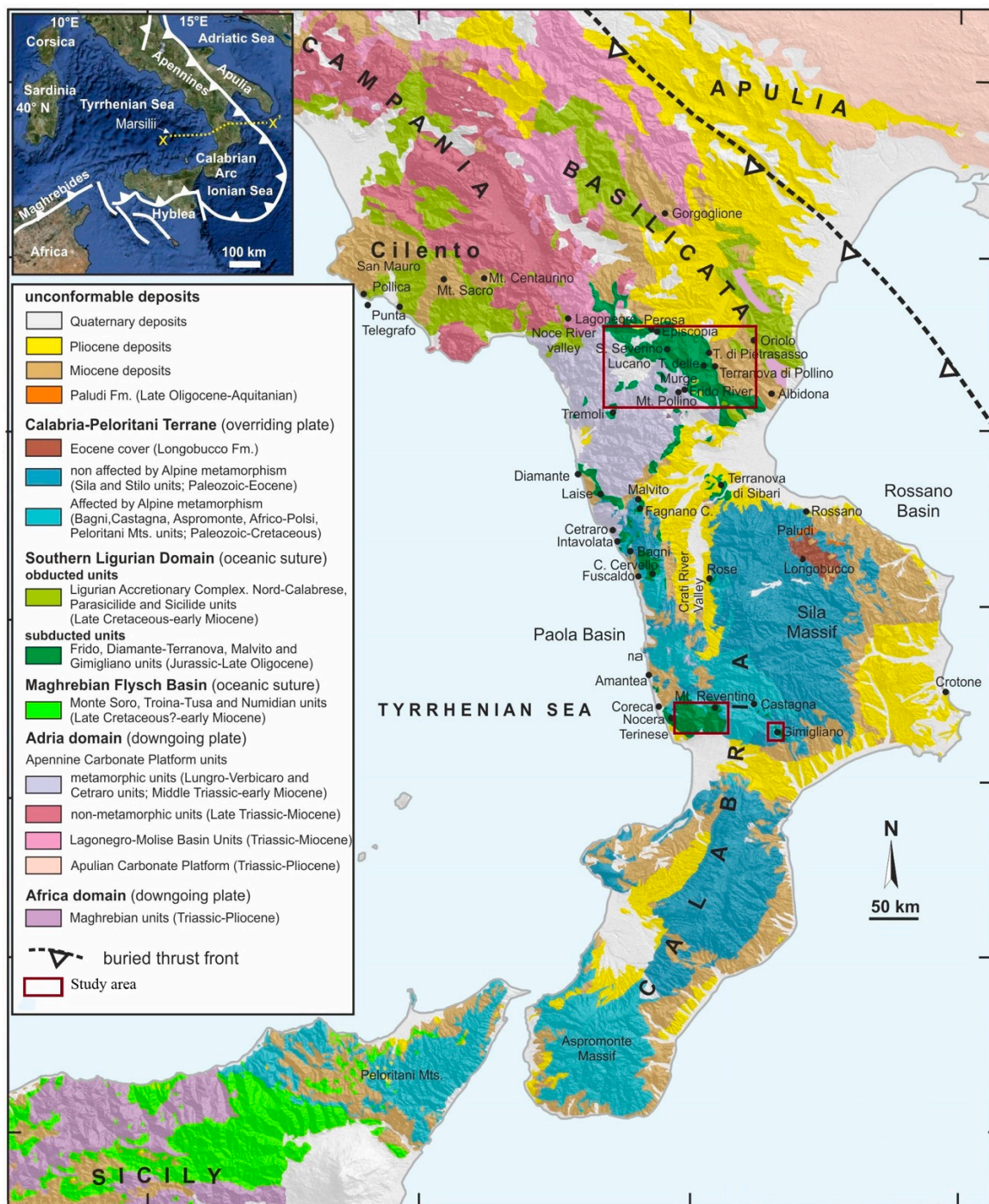
**Figure 2.** Geological sketch map of the Southern Apennines-Calabria-Peloritani chain and location of the study areas (modified after [50]).

## 3. Analytical Methods

In this paper, we report and discuss data available in literature referring to the petrographical and mineralogical studies performed on serpentinites from selected sites of southern Apennines. In particular, data here presented are from Dichicco et al. [32,33], Punturo et al. [19], Bloise et al. [5], and Campopiano et al. [20].

The petrographic characterization was carried out by optical microscopy on thin sections of rock samples. Percentages for fibrous minerals have been calculated by means of point-counting modal analysis following the EPA/600/R93-116 method. The mineralogical compositions have been obtained

by using X-ray diffraction (XRD) on bulk rock powder. Specific analyses on single minerals were performed by μ-Raman spectroscopy, FT-IR spectroscopy, SEM-EDS, and electron microprobe (EMP) analyses. Details of analytical conditions are reported in the following papers: Dichicco et al. [32,33], Punturo et al. [19], and Bloise et al. [5].

## 4. Previous Studies and New Findings

### 4.1. Asbestos Minerals in Serpentinites from the Pollino Massif

Serpentinites are characterized by an original pseudomorphic texture and mylonitic-cataclastic structures (Table 1). They are made up of fibrous minerals accounting for the 55% of the total mineral composition. The mineralogical assemblage consists of serpentine group minerals, amphibole minerals (mainly tremolite-actinolite series), titanite, clinopyroxene, clinochlore, magnetite, Cr-spinel, talc, quartz, and carbonate phases. The serpentinites are cross-cut by a micro-network of nanometer to millimeter veins filled by fibrous serpentine and serpentine ± amphiboles, amphibole minerals, and calcite ± amphiboles [32]. Chrysotile occurs as short and fine-fibers in the matrix and in the contact between vein and rock. Chrysotile occurs preferentially in serpentinites that have undergone some degree of recrystallization, in which the serpentine minerals have developed interlocking microstructures. Primary magmatic clinopyroxene occurs in partially preserved grains. The amphibole shows acicular, fibrous, and elongated habitus and forms in veins and/or in the rock matrix as crowns around the clinopyroxene porphyroclasts [32].

**Table 1.** Textural features and mineralogical assemblages of serpentinites from the study areas. Abbreviations of mineral names are from Whitney and Evans [51].

| Locality | Texture | Mineral Assemblage | Fibrous Minerals |
|---|---|---|---|
| Pollino Massif [1] | Pseudomorphic texture and mylonitic-cataclastic structures | Srp ± Mag ± Tr-Act- Ed *-Hbl ± Clc ± Cpx ± Spl ± Ttn ± Cal ± Dol ± Tlc ± Qz | Tremolite, antigorite, chrysotile, edenite* |
| Gimigliano-Mt. Reventino [2] | Protogranular texture | Srp ± Mag ± Tr-Act ± Chl ± Cpx ± Spl ± Cal ± Tlc | Tremolite, antigorite, chrysotile |

[1] Data from [32,33,52], [2] Data from [5,19–21], * This study.

Serpentine (lizardite, chrysotile, and antigorite) and amphibole-like (actinolite, d = 8.31 Å; tremolite, d = 2.94 Å) minerals have been detected by XRD analysis and represent the dominant phases of the studied samples. The 2:1 phyllosilicate (clinochlore, d = 4.74 Å) and iron oxides (magnetite, d = 2.52 Å) also occur as subordinate phases along with different types of carbonates (calcite, d = 3.04; aragonite, d = 3.38; dolomite, d= 2.88) (Table 2).

**Table 2.** Mineral assemblage of the studied serpentinites as detected by XRD, where (+ + +) = major phase, (++) = minor phase (<10%), (+) = trace phase, and (−) = absent.

| Locality | Serpentine | Magnetite | Amphibole | Carbonate | Pyroxene | Talc | Quartz | Titanite | Spinel | Clinochlore |
|---|---|---|---|---|---|---|---|---|---|---|
| Pollino Massif [1] | +++ | ++ | ++ | ++ | + | + | + | + | ++ | ++ |
| Gimigliano-Mt. Reventino [2] | +++ | + | ++ | + | + | + | − | − | + | ++ |

[1] This study, [2] Data from [5,19–21].

Serpentine group minerals were also identified by μ-Raman spectroscopy. Chrysotile is distinguished from the other minerals of the serpentine group by means of an antisymmetric band at about 3699 cm$^{-1}$, with a tail toward lower wavenumbers, and a less pronounced peak at about 3691 cm$^{-1}$ [32]. As reported by Dichicco et al. [32,33], different types of amphibole minerals also occur in the analyzed rocks. In the μ-Raman spectra of the OH vibrational region, the amphibole shows

two peaks, the most intense of which is at 3675–3673 cm$^{-1}$ (Mg; Mg; Mg), the second most intense at 3660–3663 cm$^{-1}$ (Mg; Mg; Fe). The number and relative intensity of these bands represent pure tremolite and almost pure tremolite with a small percentage of Fe$^{2+}$ (Fe-tremolite). The presence of Fe$^{2+}$ is confirmed by FT-IR [33]. No Fe$^{3+}$ is present, owing to the absence of absorption bands at Δ = 50 cm$^{-1}$ from the tremolite reference band in the FT-IR spectrum [33,52–56].

Secondary Electron observations by ESEM analyses show asbestos tremolite fibers that are straight, flexible and approximately 100 μm in length. The EDS chemical analysis shows that amphibole crystals are homogeneous, without zoning, although some crystals display different amounts of SiO$_2$, CaO, MgO, Fe$_2$O$_3$, Al$_2$O$_3$, and Na$_2$O in the rim and core [33].

The microchemical composition of most amphiboles detected by EMPA is typical of Ca-amphiboles, including tremolite and Mg-Fe-hornblende (Table 3) [56].

In addition, the EMP analysis revealed for the first time the presence of edenite in the serpentinites rocks of the Frido Unit. As shown in Figure 3, in the serpentinites of the Pollino Massif, edenite crystals grow with a fibrous habitus and form aggregates often associated with serpentine, diopside, and calcite.
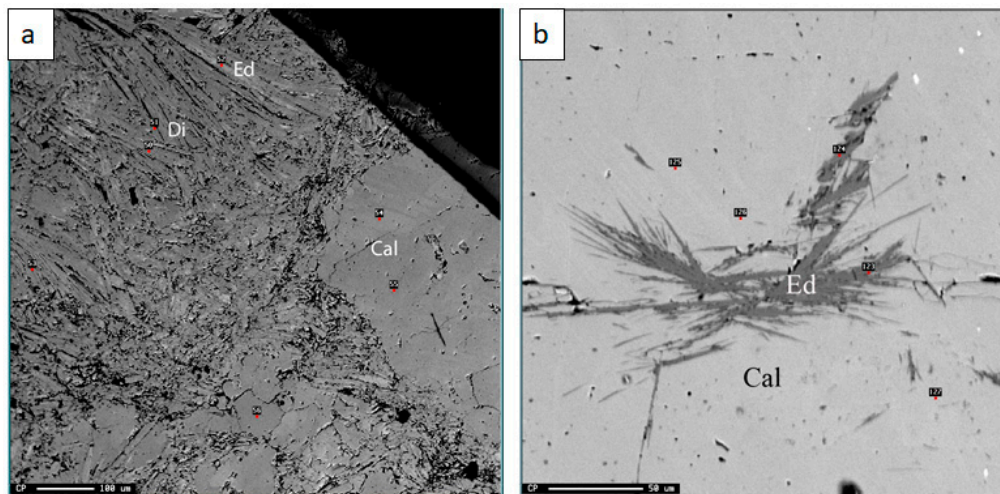


**Figure 3.** Secondary-electron image of serpentinite of the Pollino Massif showing (**a**) edenite, diopside, and calcite; (**b**) edenite crystals with both fibrous habit.

Results of the EMP analysis performed on selected fibrous crystals of edenite are shown in Table 4. Major element compositional range of this amphibole is as follows: SiO$_2$ = 51.264–54.293 wt%, CaO = 23.64–25.507 wt%, MgO = 16.332–17.680 wt%, Al$_2$O$_3$ = 0.259–2.709 wt%, and FeO$_{tot}$ = 1.257–2.852 wt% [57]. In addition, in the edenite crystals, low amounts of several trace elements, such as Mn, Cr, and Ni, are also present.

*4.2. Asbestos Minerals in Serpentinites from Gimigliano-Mt. Reventino*

The serpentinites show remnants of the original protogranular texture, which is inherited from their harzburgitic-lherzolitic protoliths [5,19]. The mineral assemblage is made of serpentine group minerals and magnetite ± tremolite-actinolite ± chlorite ± clinopyroxene ± Cr-spinel, and calcite [5,19] (Table 1). The serpentine group minerals, together with small magnetite grains, completely replaced the original olivine and orthopyroxene crystals that appear as pseudomorphic aggregates showing typical net-like and mesh textures [5,19]. According to Punturo et al. [19], clinopyroxene is in the rarely preserved holly-leaf shaped Cr-spinels that, in most cases, are quite completely retrogressed to magnetite and chlorite. Different vein systems, filled by serpentine group minerals, cross-cut the rock. In general, serpentine fibers may be oriented either perpendicular to the vein selvages ("cross" serpentine) or according to their elongation directions ("lamellar" serpentine). Minor calcite and talc flake aggregates or actinolite-tremolite fibers may occur within the serpentine matrix.

**Table 3.** Chemistry of selected fibrous tremolite and Mg-Fe-hornblende crystals in the serpentinites of the Pollino Massif.

| N. Analysis | 73 | 76 | 77 | 78 | 79 | 91 | 109 | 130 | 98 | 102 |
|---|---|---|---|---|---|---|---|---|---|---|
| Oxides (wt%) | - | - | - | - | - | - | - | - | - | - |
| $SiO_2$ | 54.588 | 57.392 | 55.674 | 52.04 | 53.735 | 57.547 | 55.015 | 57.337 | 51.657 | 55.263 |
| $P_2O_5$ | 0.031 | n.d. | n.d. | 0.01 | 0.016 | 0.028 | 0.024 | 0.057 | n.d. | 0.005 |
| $TiO_2$ | 0.158 | 0.011 | 0.059 | 0.433 | 0.268 | 0.075 | 0.059 | n.d. | 0.482 | 0.065 |
| $Al_2O_3$ | 2.798 | 0.479 | 1.559 | 5.282 | 3.543 | 1.369 | 2.509 | n.d. | 5.484 | 1.871 |
| $Cr_2O_3$ | 0.224 | 0.007 | 0.092 | 0.425 | 0.486 | 0.009 | 0.225 | n.d. | 0.502 | 0.006 |
| MnO | 0.138 | 0.089 | 0.045 | 0.026 | 0.119 | 0.082 | 0.082 | 0.022 | 0.03 | 0.17 |
| FeO | 3.925 | 3.147 | 2.475 | 3.231 | 3.064 | 2.663 | 2.401 | 2.012 | 2.871 | 7.065 |
| NiO | 0.108 | 0.09 | 0.05 | 0.082 | 0.076 | 0.045 | n.d. | n.d. | 0.139 | 0.05 |
| MgO | 23.1 | 23.415 | 24.408 | 22.602 | 23.236 | 23.524 | 23.623 | 23.445 | 21.81 | 20.999 |
| CaO | 11.427 | 13.574 | 12.845 | 11.959 | 12.063 | 12.273 | 12.523 | 13.653 | 12.421 | 9.68 |
| $Na_2O$ | 1.192 | 0.09 | 0.459 | 1.187 | 1.144 | 0.358 | 0.813 | 0.07 | 1.296 | 1.995 |
| $K_2O$ | 0.002 | n.d. | 0.014 | 0.008 | 0.014 | 0.014 | 0.016 | 0.022 | 0.028 | 0.015 |
| F | n.d. | 0.093 | n.d. | 0.039 | 0.023 | n.d. | 0.037 | 0.032 | n.d. | n.d. |
| Cl | n.d. | 0.018 | 0.019 | 0.004 | 0.02 | 0.011 | 0.006 | 0.01 | 0.027 | 0.003 |
| Sum | 97.691 | 98.362 | 97.695 | 97.311 | 97.792 | 97.996 | 97.316 | 96.645 | 96.741 | 97.186 |
| Final wt% values | | | | | | | | | | |
| MnO | 0.00 | 0.09 | 0.00 | 0.00 | 0.00 | 0.08 | 0.00 | 0.02 | 0.00 | 0.00 |
| $Mn_2O_3$ | 0.15 | 0.00 | 0.05 | 0.03 | 0.13 | 0.00 | 0.09 | 0.00 | 0.03 | 0.19 |
| FeO | 0.00 | 0.09 | 0.00 | 0.00 | 0.00 | 0.54 | 0.00 | 0.35 | 0.00 | 0.00 |
| $Fe_2O_3$ | 4.36 | 3.39 | 2.75 | 3.59 | 3.41 | 2.36 | 2.67 | 1.85 | 3.19 | 7.85 |
| $H_2O^+$ | 2.14 | 2.14 | 2.17 | 2.05 | 2.10 | 2.18 | 2.15 | 2.18 | 2.05 | 2.15 |
| Sum | 100.28 | 100.88 | 100.15 | 99.74 | 100.26 | 100.42 | 99.76 | 99.03 | 99.12 | 100.14 |
| Species | Tr | Tr | Tr | Tr | Tr | Tr | Tr | Tr | Mg-Fe-Hbl | Mg-Fe-Hbl |
| Formula Assignments T (ideally 8 apfu) | | | | | | | | | | |
| Si | 7.493 | 7.800 | 7.619 | 7.207 | 7.389 | 7.813 | 7.561 | 7.907 | 7.209 | 7.628 |
| Al | 0.453 | 0.077 | 0.251 | 0.792 | 0.574 | 0.185 | 0.406 | 0.000 | 0.791 | 0.304 |
| Ti | 0.016 | 0.001 | 0.006 | 0.000 | 0.028 | 0.000 | 0.006 | 0.000 | 0.000 | 0.007 |
| $Fe^{3+}$ | 0.036 | 0.123 | 0.123 | 0.000 | 0.008 | 0.000 | 0.025 | 0.090 | 0.000 | 0.061 |
| T subtotal | 8.000 | 8.001 | 7.999 | 8.000 | 8.000 | 8.000 | 7.999 | 8.000 | 8.000 | 8.000 |
| Formula Assignments C (ideally 5 apfu) | | | | | | | | | | |
| Cr | 0.024 | 0.001 | 0.010 | 0.047 | 0.053 | 0.001 | 0.024 | 0.000 | 0.055 | 0.001 |
| $Mn^{3+}$ | 0.016 | 0.000 | 0.005 | 0.003 | 0.014 | 0.000 | 0.010 | 0.000 | 0.004 | 0.020 |
| $Fe^{3+}$ | 0.414 | 0.225 | 0.160 | 0.374 | 0.344 | 0.241 | 0.251 | 0.102 | 0.335 | 0.755 |
| Ni | 0.012 | 0.010 | 0.006 | 0.009 | 0.008 | 0.005 | 0.000 | 0.000 | 0.016 | 0.006 |
| Mg | 4.534 | 4.744 | 4.819 | 4.452 | 4.581 | 4.711 | 4.715 | 4.820 | 4.429 | 4.219 |
| C subtotal | 5.000 | 5.001 | 5.000 | 5.000 | 5.000 | 5.000 | 5.000 | 4.965 | 5.001 | 5.001 |
| Formula Assignments B (ideally 2 apfu) | | | | | | | | | | |
| Mg | 0.193 | 0.000 | 0.160 | 0.214 | 0.182 | 0.050 | 0.125 | 0.000 | 0.108 | 0.102 |
| Ca | 1.681 | 1.977 | 1.840 | 1.775 | 1.777 | 1.785 | 1.844 | 2.000 | 1.857 | 1.432 |
| Na | 0.126 | 0.023 | 0.000 | 0.011 | 0.041 | 0.094 | 0.031 | 0.000 | 0.035 | 0.467 |
| B subtotal | 2.000 | 2.000 | 2.000 | 2.000 | 2.000 | 1.999 | 2.000 | 2.000 | 2.000 | 2.001 |
| Formula Assignments A (from 0 to 1 apfu) | | | | | | | | | | |
| Ca | 0.000 | 0.000 | 0.044 | 0.000 | 0.000 | 0.000 | 0.000 | 0.017 | 0.000 | 0.000 |
| Na | 0.191 | 0.000 | 0.122 | 0.308 | 0.264 | 0.000 | 0.186 | 0.019 | 0.316 | 0.067 |
| K | 0.000 | 0.000 | 0.002 | 0.001 | 0.002 | 0.002 | 0.003 | 0.004 | 0.005 | 0.003 |
| A subtotal | 0.191 | 0.000 | 0.168 | 0.309 | 0.266 | 0.002 | 0.189 | 0.040 | 0.321 | 0.070 |
| Sum T,C,B,A | 15.191 | 15.002 | 15.167 | 15.309 | 15.266 | 15.001 | 15.188 | 15.005 | 15.322 | 15.072 |

n.d. = not detected.

**Table 4.** Chemistry of selected fibrous edenite crystals in serpentinites samples from the Pollino Massif.

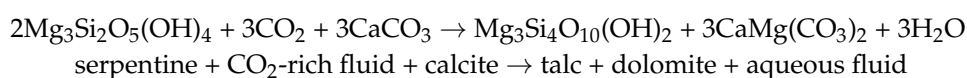| N. Analysis | 50 | 51 | 57 | 58 | 61 | 63 | 68 | 69 | 70 | 77 | 78 |
|---|---|---|---|---|---|---|---|---|---|---|---|
| Oxides (wt %) | | | | | | | | | | | |
| $SiO_2$ | 53.347 | 54.451 | 53.069 | 53.452 | 53.387 | 54.129 | 52.799 | 52.955 | 54.293 | 51.264 | 53.878 |
| $P_2O_5$ | 0.009 | 0.020 | 0.022 | 0.057 | 0.013 | 0.014 | 0.006 | 0.015 | 0.002 | 0.010 | 0.051 |
| $TiO_2$ | 0.006 | 0.006 | 0.017 | 0.025 | 0.000 | 0.012 | 0.041 | 0.012 | 0.021 | 0.002 | 0.023 |
| $Al_2O_3$ | 0.958 | 0.259 | 1.529 | 0.858 | 0.747 | 0.486 | 2.709 | 0.785 | 0.382 | 1.869 | 0.388 |
| $Cr_2O_3$ | 0.015 | 0.000 | 0.016 | 0.000 | 0.024 | 0.013 | 0.000 | 0.006 | 0.003 | 0.000 | 0.007 |
| MnO | 0.151 | 0.061 | 0.184 | 0.082 | 0.036 | 0.124 | 0.120 | 0.124 | 0.137 | 0.147 | 0.124 |
| FeO | 1.257 | 1.269 | 2.303 | 1.767 | 1.342 | 1.852 | 2.233 | 1.961 | 1.435 | 2.037 | 2.852 |
| NiO | 0.014 | 0.043 | 0.000 | 0.050 | 0.061 | 0.000 | 0.000 | 0.048 | 0.026 | 0.000 | 0.010 |
| MgO | 17.680 | 17.076 | 16.512 | 16.917 | 17.506 | 16.720 | 16.332 | 16.704 | 17.101 | 17.066 | 16.990 |
| CaO | 23.640 | 25.340 | 24.529 | 24.833 | 24.716 | 25.228 | 24.079 | 24.949 | 25.507 | 24.555 | 25.405 |
| $Na_2O$ | 0.102 | 0.057 | 0.145 | 0.091 | 0.071 | 0.076 | 0.118 | 0.062 | 0.102 | 0.040 | 0.056 |
| $K_2O$ | 0.046 | 0.028 | 0.036 | 0.037 | 0.007 | 0.000 | 0.014 | 0.026 | 0.000 | 0.018 | 0.005 |
| F | 0.000 | 0.000 | 0.014 | 0.000 | 0.000 | 0.024 | 0.020 | 0.000 | 0.000 | 0.013 | 0.000 |
| Cl | 0.023 | 0.016 | 0.073 | 0.028 | 0.014 | 0.011 | 0.016 | 0.002 | 0.013 | 0.013 | 0.007 |
| Sum | 97.24 | 98.63 | 98.43 | 98.19 | 97.92 | 98.68 | 98.48 | 97.65 | 99.02 | 97.02 | 99.80 |
| Final wt % values | | | | | | | | | | | |
| $Mn_2O_3$ | 0.17 | 0.07 | 0.21 | 0.09 | 0.04 | 0.14 | 0.13 | 0.14 | 0.15 | 0.16 | 0.14 |
| $Fe_2O_3$ | 1.40 | 1.41 | 2.56 | 1.96 | 1.49 | 2.06 | 2.48 | 2.18 | 1.60 | 2.26 | 3.17 |
| $H_2O^+$ | 2.12 | 2.11 | 2.08 | 2.10 | 2.11 | 2.10 | 2.09 | 2.10 | 2.10 | 2.09 | 2.09 |
| Sum | 99.52 | 100.88 | 100.79 | 100.49 | 100.19 | 101.00 | 100.83 | 99.98 | 101.30 | 99.36 | 102.22 |
| Species | Ed | Ed | Ed | Ed | Ed | Ed | Ed | Ed | Ed | Ed | Ed |
| Formula Assignments T (ideally 8 apfu) | | | | | | | | | | | |
| Si | 7.573 | 7.647 | 7.485 | 7.552 | 7.553 | 7.607 | 7.421 | 7.532 | 7.605 | 7.351 | 7.516 |
| P | 0.001 | 0.001 | 0.001 | 0.003 | 0.001 | 0.001 | n.d. | 0.001 | n.d. | 0.001 | 0.003 |
| Al | 0.160 | 0.043 | 0.254 | 0.143 | 0.125 | 0.080 | 0.449 | 0.132 | 0.063 | 0.316 | 0.064 |
| Ti | 0.001 | 0.001 | 0.002 | 0.003 | n.d. | 0.001 | 0.004 | 0.001 | 0.002 | n.d. | 0.002 |
| $Fe^{3+}$ | 0.149 | 0.149 | 0.258 | 0.209 | 0.159 | 0.218 | 0.126 | 0.233 | 0.168 | 0.244 | 0.333 |
| T subtotal | 7.884 | 7.841 | 8.000 | 7.910 | 7.838 | 7.907 | 8.000 | 7.899 | 7.838 | 7.912 | 7.918 |
| Formula Assignments C (ideally 5 apfu) | | | | | | | | | | | |
| Cr | 0.002 | n.d. | 0.002 | n.d. | 0.003 | 0.001 | n.d. | 0.001 | n.d. | n.d. | 0.001 |
| $Mn^{3+}$ | 0.018 | 0.007 | 0.022 | 0.010 | 0.004 | 0.015 | 0.014 | 0.015 | 0.016 | 0.018 | 0.015 |
| $Fe^{3+}$ | n.d. | n.d. | 0.014 | n.d. | n.d. | n.d. | 0.137 | n.d. | n.d. | n.d. | n.d. |
| Ni | 0.002 | 0.005 | n.d. | 0.006 | 0.007 | n.d. | n.d. | 0.005 | 0.003 | n.d. | 0.001 |
| Mg | 3.742 | 3.575 | 3.472 | 3.563 | 3.692 | 3.503 | 3.422 | 3.542 | 3.571 | 3.648 | 3.533 |
| C subtotal | 3.764 | 3.587 | 3.510 | 3.579 | 3.706 | 3.519 | 3.573 | 3.563 | 3.590 | 3.666 | 3.550 |
| Formula Assignments B (ideally 2 apfu) | | | | | | | | | | | |
| Ca | 2.000 | 2.000 | 2.000 | 2.000 | 2.000 | 2.000 | 2.000 | 2.000 | 2.000 | 2.000 | 2.000 |
| B subtotal | 2.000 | 2.000 | 2.000 | 2.000 | 2.000 | 2.000 | 2.000 | 2.000 | 2.000 | 2.000 | 2.000 |
| Formula Assignments A (from 0 to 1 apfu) | | | | | | | | | | | |
| Ca | 1.596 | 1.813 | 1.707 | 1.759 | 1.747 | 1.799 | 1.626 | 1.802 | 1.828 | 1.773 | 1.797 |
| Na | 0.028 | 0.016 | 0.040 | 0.025 | 0.019 | 0.021 | 0.032 | 0.017 | 0.028 | 0.011 | 0.015 |
| K | 0.008 | 0.005 | 0.006 | 0.007 | 0.001 | n.d. | 0.003 | 0.005 | n.d. | 0.003 | 0.001 |
| A subtotal | 1.632 | 1.834 | 1.753 | 1.791 | 1.767 | 1.820 | 1.661 | 1.824 | 1.856 | 1.787 | 1.813 |
| Sum T,C,B,A | 15.280 | 15.262 | 15.263 | 15.280 | 15.311 | 15.246 | 15.234 | 15.286 | 15.284 | 15.365 | 15.281 |

n.d. = not detected.

The X-ray diffraction analysis revealed that these rocks are mainly constituted of serpentine group minerals, followed by chlorite and tremolite [5,19] (Table 2). Calcite was detected less frequently and in low amounts. μ-Raman spectroscopy identified chrysotile, lizardite, and antigorite. In the spectral region associated with the structural bending characterization, serpentine group minerals are characterized by very similar μ-Raman spectra. In chrysotile, the characteristic ν5 (e) bending vibrations of the $SiO_4$ tetrahedra are shown at 388 and 344 $cm^{-1}$. Lizardite shows a very similar pattern to chrysotile [5], whereas antigorite displays a characteristic band occurring at 1042 $cm^{-1}$ and an intense band at 683 $cm^{-1}$. The two bands observed at 378 and 634 $cm^{-1}$ appear to be slightly shifted when compared with the same vibrations present in the chrysotile spectrum [5]. Similarly to the serpentinites of the Pollino Massif, the tremolite of Gimigliano-Mt. Reventino rocks is characterized by the presence only of $Fe^{2+}$ detected by FT-IR analysis [57]. The $Fe^{3+}$ presence is excluded because of the absence of the absorption bands at $\Delta = -50$ $cm^{-1}$. Further, the FT-IR and SEM-EDS analyses confirmed the presence of antigorite, chrysotile, and fibrous minerals, from the tremolite–actinolite series, in the samples from Mt. Reventino [20,21,58].

## 5. Discussion and Conclusions

Data presented in this study display a very similar mineralogical composition for both the considered serpentinites including serpentine group minerals, amphiboles, pyroxene, chlorite, talc, titanite, magnetite, and carbonates. However, compared to the serpentinites from Northern Calabria, the Pollino Massif serpentinites are characterized also by the presence of quartz, dolomite, and edenite.

Based on textural and mineralogical data, quartz and dolomite are always found in association with, talc likely suggesting their formation during a metasomatic event. According to Boschi et al. [59], in fact, serpentine minerals may easily alter to talc + dolomite assemblage as the following reaction:

$$2Mg_3Si_2O_5(OH)_4 + 3CO_2 + 3CaCO_3 \rightarrow Mg_3Si_4O_{10}(OH)_2 + 3CaMg(CO_3)_2 + 3H_2O$$

serpentine + $CO_2$-rich fluid + calcite → talc + dolomite + aqueous fluid

Instead, quartz may be thought as the result of the direct precipitation from migrating fluids that, as stated by Moore and Rymer [60], may become enriched with dissolved silica during the alteration of serpentine and other primary silicates of mafic and ultramafic rocks.

As regards edenite, the presence of such a mineral within the serpentinitic rocks from the ophiolitic sequence of Southern Apennines is documented here for the first time. Edenite is a double chain silicate mineral of the amphibole group with the following general formula: $NaCa_2(Mg,Fe)_5[Si_7AlO_{22}](OH)_2$ [61]. This is a rare mineral in the ophiolitic sequences although its presence has been documented in the oceanic serpentinites from the Mid-Atlantic Ridge and the Greater Antilles (Cuba, Dominican Republic) [62,63], where it testifies a medium to high metamorphism. As suggested by Bucher and Frey [64], the edenite formation is linked to the greenschist-amphibolite facies transition. In particular, such a mineral is produced by albite-consuming reactions in volcanic rocks, as albite + tremolite = edenite + 4 quartz, or in basic rocks, as olivine + labradorite + $H_2O$ = ortopyroxene + edenite + spinel [61], and occurs during metamorphic events that promote systematic changes of the amphibole composition (from tremolite to edenite).

However, metasomatic processes not correlated to metamorphism can also be responsible for the formation of edenite or (more commonly) fluoro-edenite crystals. The F-edenite of Biancavilla, a village located in the etnean volcanic complex of Eastern Sicily (Southern Italy), is an example of an amphibole not metamorphic in origin. According to Comba et al. [65], the Sicilian F-edenite is found in voids and fractures of the benmoreitic lava covering the Mt. Calvario or in highly weathered pyroclastic products and scoriae that have been involved by metasomatizing hot fluids during volcanism or processes linked to it.

Regardless of process promoting edenite formation, it is worth noting that this amphibole, similarly to the more common asbestos minerals, may crystallize with fibrous habit and thus could

represent a mineral harmful for human health, although edenite is currently not regulated by the Directive 2003/18/EC of the European Parliament either by the European Council of 27th March 2003. In addition, our data highlight that edenite crystals host different types of trace metals that could increase their toxicity as suggested by Bloise et al. [13] for the other asbestos minerals.

As a consequence, we believe that further detailed field and laboratory investigations are needed to improve our knowledge on edenite formation in the serpentinitic rocks of the Southern Apennines in order to better constrain the mode of occurrence of this "potentially harmful" mineral at the Pollino Massif.

## References

1. Belluso, E.; Compagnoni, R.; Ferraris, G. *Occurrence of Asbestiform Minerals in the Serpentinites of the Piemonte Zone, Western Alps*; Giornata di Studio in ricordo del Prof. Stefano Zucchetti; Politecnico di Torino: Torino, Italy, 1994; pp. 57–64.

2. Groppo, C.; Rinaudo, C.; Cairo, S.; Gastaldi, D.; Compagnoni, R. Micro-Raman spectroscopy for a quick and reliable identification of serpentine minerals from ultramafics. *Eur. J. Mineral.* **2006**, *18*, 319–329. [CrossRef]

3. Hendrickx, M. Naturally occurring asbestos in eastern Australia: A review of geological occurrence, disturbance and mesothelioma risk. *Environ. Geol.* **2009**, *57*, 909–926. [CrossRef]

4. Vignaroli, G.; Ballirano, P.; Belardi, G.; Rossetti, F. Asbestos fibre identification vs. evaluation of asbestos hazard in ophiolitic rock mélanges, a case study from the Ligurian Alps (Italy). *Environ. Earth Sci.* **2013**, *72*, 3679–3698. [CrossRef]

5. Bloise, A.; Punturo, R.; Catalano, M.; Miriello, D.; Cirrincione, R. Naturally occurring asbestos (NOA) in rock and soil and relation with human activities: The monitoring example of selected sites in Calabria (southern Italy). *Ital. J. Geosci.* **2016**, *135*, 268–279. [CrossRef]

6. Virta, R.L. *Mineral Commodity Profiles: Asbestos*; USGS Circular 1255-KK; US Geological Survey (USGS): Reston, VA, USA, 2005; p. 56.

7. Nichols, M.D.; Young, D.; Davis, G. *Guidelines for Geologic Investigations of Naturally Occurring Asbestos in California*; Special publication; California Geological Survey Public Information Offices: Los Angeles, CA, USA, 2002; p. 124.

8. IARC Working Group on the Evaluation of Carcinogenic Risks to Humans, and World Health Organization. *Overall Evaluations of Carcinogenicity: An Updating of IARC Monographs*; World Health Organization: Geneva, Switzerland, 1987; Volume 1–42.

9. Mossman, B.T.; Lippmann, M.; Hesterberg, T.W.; Kelsey, K.T.; Barchowsky, A.; Bonner, J.C. Pulmonary endpoints (lung carcinomas and asbestosis) following inhalation exposure to asbestos. *J. Toxicol. Environ. Health* **2011**, *14*, 76–121. [CrossRef] [PubMed]

10. Bloise, A.; Belluso, E.; Barrese, E.; Miriello, D.; Apollaro, C. Synthesis of Fe-doped chrysotile and characterization of the resulting chrysotile fibres. *Cryst. Res. Technol.* **2009**, *44*, 590–596. [CrossRef]

11. Bloise, A.; Barrese, E.; Apollaro, C.; Miriello, D. Flux growth and characterization of Ti- and Ni-doped forsterite single crystals. *Cryst. Res. Technol* **2009**, *44*, 463–468. [CrossRef]

12. Bloise, A.; Belluso, E.; Fornero, E.; Rinaudo, C.; Barrese, E.; Cappella, S. Influence of synthesis condition on growth of Ni-doped chrysotile. *Microporous Mesoporous Mater.* **2010**, *132*, 239–245. [CrossRef]

13. Bloise, A.; Barca, D.; Gualtieri, A.F.; Pollastri, S.; Belluso, E. Trace elements in hazardous mineral fibres. *Environ. Pollut.* **2016**, *216*, 314–323. [CrossRef] [PubMed]

14. Loreto, C.; Carnazza, M.L.; Cardile, V.; Libra, M.; Lombardo, L.; Malaponte, G.; Martinez, G.; Musumeci, G.; Papa, V.; Cocco, L. Mineral fiber-mediated activation of phosphoinositide-specific phospho-lipase c in human bronchoalveolar carcinoma-derived alveolar epithelial A549 cells. *Int. J. Oncol.* **2009**, *34*, 371–376.

15. Pugnaloni, A.; Giantomassi, F.; Lucarini, G.; Capella, S.; Bloise, A.; Di Primo, R.; Belluso, E. Cytotoxicity induced by exposure to natural and synthetic tremolite asbestos: An in vitro pilot study. *Acta Histochem.* **2013**, *115*, 100–112. [CrossRef] [PubMed]

16. Gueguen, E.; Doglioni, C.; Fernandez, M. On the post-25 Ma geodynamic evolution of the western Mediterranean. *Tectonophysics* **1998**, *298*, 259–269. [CrossRef]

17. Cello, G.; Mazzoli, S. Apennine tectonics in southern Italy: A review. *J. Geodyn.* **1999**, *27*, 191–211. [CrossRef]

18. Doglioni, C.; Gueguen, E.; Harabaglia, P.; Mongelli, F. On the origin of west-directed subduction zones and applications to the western Mediterranean. In *The Mediterranean Basins: Tertiary Extension within the Alpine Orogen*; Durand, B., Jolivet, L., Horváth, F., Séranne, M., Eds.; Special Publications Geological Society: London, UK, 1999; Volume 156, pp. 541–561.

19. Punturo, R.; Bloise, A.; Critelli, T.; Catalano, M.; Fazio, E.; Apollaro, C. Environmental implications related to natural asbestos occurrences in the ophiolites of the Gimigliano-Mount Reventino Unit (Calabria, Southern Italy). *Int. J. Environ. Res.* **2015**, *9*, 405–418.

20. Campopiano, A.; Olori, A.; Spadafora, A.; Rosaria Bruno, M.; Angelosanto, F.; Iannò, A.; Iavicoli, S. Asbestiform minerals in ophiolitic rocks of Calabria (southern Italy). *Int. J. Environ. Health Res.* **2018**, *28*, 134–146. [CrossRef] [PubMed]

21. Apollaro, C.; Fuoco, I.; Vespasiano, G.; De Rosa, R.; Cofone, F.; Miriello, D.; Bloise, A. Geochemical and mineralogical characterization of tremolite asbestos contained in the Gimigliano-Mount Reventino Unit (Calabria, south Italy). *J. Mediterr. Earth Sci.* **2018**, *1*, 5–15.

22. Knott, S.D. The Liguride Complex of southern Italy—A Cretaceous to Paleogene accretionary wedge. *Tectonophysics* **1987**, *142*, 217–226. [CrossRef]

23. Knott, S.D. Structure, kinematics and metamorphism of the Liguride complex, southern Apennines, Italy. *J. Struct. Geol.* **1994**, *16*, 1107–1120. [CrossRef]

24. Monaco, C.; Tansi, C.; Tortorici, L.; De Francesco, A.M.; Morten, L. Analisi geologico-strutturale dell'Unità del Frido al confine calabro-lucano (Appennino Meridionale). *Mem. Soc. Geol. Ital.* **1991**, *47*, 341–353.

25. Monaco, C.; Tortorici, L. Tectonic role of ophiolite-bearing terranes in building of the Southern Apennines orogenic belt. *Terra Nova* **1995**, *7*, 153–160. [CrossRef]

26. Cirrincione, R.; Monaco, C. Evoluzione tettonometamorfica dell'Unità del Frido (Appennino Meridionale). *Mem. Soc. Geol. Ital.* **1996**, *51*, 83–92.

27. Tortorici, L.; Catalano, S.; Monaco, C. Ophiolite-bearing melanges in southern Italy. *Geol. J.* **2009**, *44*, 153–166. [CrossRef]

28. Sansone, M.T.C.; Rizzo, G.; Mongelli, G. Petrochemical characterization of mafic rocks from Ligurian ophiolites, southern Apennines. *Int. Geol. Rev.* **2011**, *53*, 130–156. [CrossRef]

29. Laurita, S.; Prosser, G.; Rizzo, G.; Langone, A.; Tiepolo, M.; Laurita, A. Geochronological study of zircons from continental crust rocks in the Frido Unit (Southern Apennines). *Int. J. Earth Sci.* **2014**, *104*, 179–203. [CrossRef]

30. Dichicco, M.C.; Laurita, S.; Paternoster, M.; Rizzo, G.; Sinisi, R.; Mongelli, G. Serpentinite Carbonation for $CO_2$ Sequestration in the Southern Apennines: Preliminary Study. *Energy Procedia* **2015**, *76*, 477–486. [CrossRef]

31. Dichicco, M.C.; De Bonis, A.; Mongelli, G.; Rizzo, G.; Sinisi, R. Naturally occurring asbestos in the southern Apennines: Quick μ-Raman Spectroscopy identification as a tool of environmental control. In Proceedings of the 13th International Conference on Protection and Restoration of the Environment, Mykonos Island, Greece, 3–8 July 2016.

32. Dichicco, M.C.; De Bonis, A.; Mongelli, G.; Rizzo, G.; Sinisi, R. μ-Raman spectroscopy and X-ray diffraction of asbestos' minerals for geo-environmental monitoring: The case of the southern Apennines natural sources. *Appl. Clay Sci.* **2017**, *141*, 292–299. [CrossRef]

33. Dichicco, M.C.; Laurita, S.; Sinisi, R.; Battiloro, R.; Rizzo, G. Environmental and Health: The Importance of Tremolite Occurence in the Pollino Geopark (Southern Italy). *Geosciences* **2018**, *8*, 98. [CrossRef]

34. Dichicco, M.C.; Castiñeiras, P.; Galindo Francisco, C.; González Acebrón, L.; Grassa, F.; Laurita, S.; Paternoster, M.; Rizzo, G.; Sinisi, R.; Mongelli, G. Genesis of carbonate-rich veins in the serpentinites

at the Calabria-Lucania boundary (southern Apennines). *Rend. Online Soc. Geol. Ital.* **2018**, *44*, 143–149. [CrossRef]

35. Rizzo, G.; Laurita, S.; Altenberger, U. The Timpa delle Murge ophiolitic gabbros, southern Apennines: Insights from petrology and geochemistry and consequences to the geodynamic setting. *Period. Mineral.* **2018**, *87*, 5–20.

36. Mazzeo, F.C.; Zanetti, A.; Aulinas, M.; Petrosino, M.; Arienzo, I.; D'Antonio, M. Evidence for an intra-oceanic affinity of the serpentinized peridotites from the Mt. Pollino ophiolites (southern Ligurian Tethys): Insights into the peculiar tectonic evolution of the southern Apennines. *Lithos* **2017**, *284*, 367–380. [CrossRef]

37. Vitale, S.; Fedele, L.; Tramparulo, F.; Ciarcia, S.; Mazzoli, S.; Novellino, A. Structural and petrological analyses of the Frido Unit (southern Italy): New insights into the early tectonic evolution of the southern Apennines-Calabrian Arc system. *Lithos* **2013**, *168–169*, 219–235. [CrossRef]

38. Sansone, M.T.C.; Prosser, G.; Rizzo, G.; Tartarotti, P. Spinel peridotites of the Frido unit ophiolites (southern Apennines Italy): Evidence for oceanic evolution. *Period Miner.* **2012**, *81*, 35–59.

39. Sansone, M.T.C.; Tartarotti, P.; Prosser, G.; Rizzo, G. From ocean to subduction: The polyphase metamorphic evolution of the Frido unit metadolerite dykes (southern Apennine, Italy). Multiscale structural analysis devoted to the reconstruction of tectonic trajectories in active margins. *J. Virtual. Explor. Electron. Ed.* **2012**, *41*, 3.

40. Sansone, M.T.C.; Rizzo, G. Pumpellyite veins in the metadolerite of the Frido unit (southern Apennines-Italy). *Period. Mineral.* **2012**, *81*, 75–92.

41. Spadea, P. Calabria-Lucania ophiolites. *Boll. Geofis. Teorica Appl.* **1994**, *36*, 271–281.

42. Laurita, S.; Rizzo, G. Blueschist metamorphism of metabasite dykes in the serpentinites of the Frido Unit, Pollino Massif. *Rend. Online Soc. Geol. Ital.* **2018**, *45*, 129–135. [CrossRef]

43. Alvarez, W. Structure of the Monte Reventino greenschist folds: A contribution to untangling the tectonic-transport history of Calabria, a key element in Italian tectonics. *J. Struct. Geol.* **2005**, *27*, 1355–1378. [CrossRef]

44. Liberi, F.; Piluso, E. Tectonometamorphic evolution of the ophiolites sequences from Northen Calabrian Arc. *Ital. J. Geosci.* **2009**, *128*, 483–493.

45. Ogniben, L. Schema introduttivo alla geologia del confine calabro-lucano. *Mem. Soc. Geol. Ital.* **1969**, *8*, 453–763.

46. Ogniben, L. Schema Geologico della Calabria in base ai dati odierni. *Geol. Rom.* **1973**, *XII*, 243–585.

47. Piluso, E.; Cirrincione, R.; Morten, L. Ophiolites of the Calabrian Peloritani Arc and their relationships with the Crystalline Basement, Catena Costiera and Sila Piccola, Calabria, Southern Italy. *GLOM 2000 Excursion Guide-Book* **2000**, *25*, 117–140.

48. Pezzino, A.; Angì, G.; Fazio, E.; Fiannacca, P.; Lo Giudice, A.; Ortolano, G.; Punturo, R.; Cirrincione, R.; De Vuono, E. Alpine metamorphism in the aspromonte massif: Implications for a new framework for the southern sector of the Calabria-Peloritani Orogen, Italy. *Int. Geol. Rev.* **2008**, *50*, 423–441. [CrossRef]

49. Cirrincione, R.; Fazio, E.; Heilbronner, R.; Kern, H.; Mengel, K.; Ortolano, G.; Pezzino, A.; Punturo, R. Microstructure and elastic anisotropy of naturally deformed leucogneiss from a shear zone in Montalto (southern Calabria, Italy). *Geol. Soc. Lond. Spec. Publ.* **2010**, *332*, 49–68. [CrossRef]

50. Vitale, S.; Ciarcia, S.; Fedele, L.; Tramparulo, F. The Ligurian oceanic successions in southern Italy: The key to decrypting the first orogenic stages of the southern Apennines-Calabria chain system. *Tectonophysics* **2018**. [CrossRef]

51. Whitney, D.L.; Evans, B.W. Abbreviations for names of rock-forming minerals. *Am. Mineral.* **2010**, *95*, 185–187. [CrossRef]

52. Dichicco, M.C. Genesis of Carbonate-Rich Veins in the Serpentinites Outcropping at the Calabria-Lucania Boundary (Southern Apennines). Ph.D. Thesis, University of Basilicata, Potenza, Italy, 10 April 2018, unpublished.

53. Raudsepp, M.; Turnock, A.C.; Hawthorne, F.C.; Sherriff, B.L.; Hartman, J.S. Characterization of synthetic pargasitic amphiboles ($NaCa_2Mg_4M^{3+}Si_6Al_2O_{22}(OH, F)_2$; $M^{3+}$ = Al, Cr, Ga, Fe, Sc, In) by infrared spectroscopy, Rietveld structure refinement, and $^{27}Al$, $^{29}Si$, and $^{19}F$ MAS NMR spectroscopy. *Am. Mineral.* **1987**, *72*, 580–593.

54. Ballirano, P.; Andreozzi, G.B.; Belardi, G. Crystal chemical and structural characterization of fibrous tremolite from Susa Valley, Italy, with comments on potential harmful effects on human health. *Am. Mineral.* **2008**, *93*, 1349–1355. [CrossRef]

55. Pacella, A.; Ballirano, P.; Cametti, G. Quantitative chemical analysis of erionite fibres using a micro-analytical SEM-EDX method. *Eur. J. Mineral.* **2016**, *28*, 257–264. [CrossRef]

56. Dichicco, M.C.; Laurita, S.; Mongelli, G.; Rizzo, G.; Sinisi, R. Environmental problems related to serpentinites in the Pollino Geopark (Southern Appennine). In *89° Congresso congiunto SGI-SIMP, Rendiconti Online*; Società Geologica Italiana: Catania, Italy, 2018; p. 578.

57. Skogby, H.; Rossman, G.R. The intensity of amphibole OH bands in the infrared absorption spectrum. *Phys. Chem. Miner.* **1991**, *18*, 64–68. [CrossRef]

58. Campopiano, A.; Olori, A.; Cannizzaro, A.; Ianno, A.; Capone, P.P. Quantification of tremolite in friable material coming from Calabrian ophiolitic deposits by infrared spectroscopy. *J. Spectroscop.* **2015**, *2015*, 974902. [CrossRef]

59. Boschi, C.; Früh-Green, G.L.; Escartín, J. Occurrence and significance of serpentinite-hosted, talc-and amphibole-rich fault rocks in modern oceanic settings and ophiolite complexes: An overview. *Ofioliti* **2006**, *31*, 129–140.

60. Moore, D.E.; Rymer, M.J. Talc-bearing serpentinite and the creeping section of the San Andreas fault. *Nature* **2007**, *448*, 795. [CrossRef]

61. Deer, W.A.; Howie, R.A.; Zussman, H.J. *Introduzione ai Minerali che Costituiscono le Rocce*; Zanichelli Editore S.P.A.: Modena, Italy, 1994.

62. Garcìa-Casco, A.; Torres-Roldán, R.L.; Milla, G.; Millán, P.; Schneider, J. Oscillatory zoning in eclogitic garnet and amphibole, Northern Serpentinite Melange, Cuba: A record of tectonic instability during subduction? *J. Metamorph. Geol.* **2002**, *20*, 581–598. [CrossRef]

63. Deschamps, F.; Guillot, S.; Godard, M.; Andreani, M.; Hattori, K. Serpentinites act as sponges for fluid-mobile elements in abyssal and subduction zone environments. *Terra Nova* **2011**, *23*, 171–178. [CrossRef]

64. Bucher, K.; Frey, M. *Petrogenesis of Metamorphic Rocks*; Springer-Verlag: Berlin, Germany, 2002; 341p.

65. Comba, P.; Gianfagna, A.; Paoletti, L. Pleural Mesothelioma Cases in Biancavilla are Related to a New Fluoro-Edenite Fibrous Amphibole. *Arch. Environ. Health Int. J.* **2003**, *58*, 229–232. [CrossRef]